Available online at www.sciencedirect.com
SCIENCE DIRECT
Polymer 46 (2005) 3077–3089
polymer
www.elsevier.com/locate/polymer

The effect of storage of poly(propylene) pipes under hydrostatic pressure and elevated temperatures on the morphology, molecular mobility and failure behaviour

V.M. Litvinov[a,*], M. Soliman[b]

[a]DSM Research, Resolve, P.O. Box 18, 6160 MD Geleen, The Netherlands
[b]SABIC EuroPetrochemicals, P.O. Box 319, 6160 AH Geleen, The Netherlands

Received 10 August 2003; received in revised form 12 December 2004; accepted 27 January 2005
Available online 9 March 2005

Abstract

One of the important applications of random poly(ethylene propylene) copolymer (PPR) is the production of hot water pipes. The pipes can be used under hydrostatic pressure as well as at elevated temperatures up to 70 °C continuously for 50 years and at short time at 80 °C. If a pipe is used at higher temperatures for longer times it could fail earlier. Knowledge of usage time and temperature is vital for determining the origin of a failure of PPR pipes. Several techniques are used for determining changes in chemical and physical structures upon long-time annealing of PPR pipes at different temperatures. Techniques, which are sensitive to thermo-oxidative degradation of PPR and consumption of stabilizers, are not very sensitive for determining storage time longer than one year. The molar mass of PPR does not change upon long-time annealing. It is shown that crystallinity of the samples, as determined by wide angle X-ray diffraction (WAXD), is not largely affected by storage time at elevated temperatures. It is also shown that onset of melting, as measured by differential scanning calorimetry (DSC), increases with increasing storage temperature, which is apparently caused by the perfection of crystalline structure at higher temperatures. Onset of melting allows determining the maximum storage temperature of PPR pipes. It is shown that proton solid-state NMR transverse magnetization (T_2) relaxation analysis is the most sensitive tool for determining changes in PPR samples that are caused by storage time of PPR pipes under hydrostatic pressure. The method provides information on molecular mobility and phase composition of PPR samples. Four different phases are analysed with this method: (1) crystalline phase and rigid fraction of the amorphous phase, (2) semi-rigid crystal-amorphous interface, (3) soft fraction of the amorphous phase and (4) rubbery-like material. The most pronounced changes upon long storage time are observed for the rigid fraction of PPR (fraction 1). This suggests that long time annealing of the samples at temperatures far above T_g (about 0 °C) results in (1) perfection of existing crystals and the formation of new crystals, which act as physical junctions leading to immobilization of the amorphous phase, (2) chain elongation in the amorphous phase due to creep under hydrostatic pressure, and (3) an increase in the gradient of concentration of ethylene-rich chain fragments through the mobile fractions of the amorphous phase. All these changes cause embrittlement of the samples. Thus, the combination of DSC and solid-state NMR measurements is a powerful tool for determining the critical time and temperature conditions causing breakage of PPR pipes and fittings.

Keywords: Proton solid-state NMR relaxation; The phase composition; Molecular mobility

1. Introduction

One of the important applications of random poly(ethylene propylene) copolymer (PPR) is the production of hot water pipes in sanitary applications. According to the product specification, the pipes can be used under hydrostatic pressure (between 3 and 15 bar depending on the height of the building) and at elevated temperatures up to 70 °C continuously for 50 years and for a short time (all together 1 year) at 80 °C. Physical ageing and creep phenomena occur at elevated temperatures under hydrostatic pressure, which can cause pipe breakage, if ageing time at a certain temperature exceeds that of the specification. In this case, the product quality is not guaranteed. In this respect the question arises, how we can determine the

* Corresponding author. Tel.: +31 46 4761256; fax: +31 46 4761200.
E-mail address: victor.litvinov@dsm.com (V.M. Litvinov).

0032-3861/$ - see front matter © 2005 Elsevier Ltd. All rights reserved.
doi:10.1016/j.polymer.2005.01.074

time and temperature of usage of pipes made from random polypropylene (PPR)?

In order to meet the demand of continuous use for 50 years at 70 °C under pressure, the material has to combine good thermal stability with an intrinsic creep resistance. This combination is reached by using PPR with a very high molecular weight containing certain additives that prevent thermo-oxidative degradation. PPR has a higher creep resistance at higher temperatures and hydrostatic pressure than homopolymer polypropylene (PPH) or block copolymer of PP with a rubber (PPB). The higher pressure resistance of PPR can be explained by the higher amount of efficient tie chains in PPR due to ethylene chain fragments disturbing the formation of large crystals. Therefore, each chain can be built in a larger number of crystals than this would be possible in a PPH. This results in a tighter physical network in the amorphous phase of PPR. An increase in molecular weight of PPR also improves the creep resistance due to a larger connectivity of crystals.

Although PPR is a very suitable material for long-lasting hot water pipes, it is still possible that a pipe could break. In order to improve the performance of pipes, knowledge of the molecular origin of the fracture behaviour is necessary. Long storage time at elevated temperatures and hydrostatic pressure causes changes in the chemical structure due to thermal oxidative degradation and in physical structures. A number of techniques are used in the present study to determine these changes as a function of storage time at different temperatures.

The degree of chemical degradation is studied by measuring the remaining amount of long-term stabilizers, molar mass of PPR, by determining the stability of a used pipe with oven ageing experiments, and using the so-called oxidation induction time which is also related to the thermal stability of a sample. Several techniques are applied for determining changes in physical properties upon storage time, i.e. the degree of crystallinity is studied with WAXD, melting behaviour is studied with DSC, dynamic mechanical thermal analysis (DMTA) is used for analysing mechanical properties and solid-state NMR is used to measure changes in the molecular mobility and the phase composition.

2. Experimental

2.1. PPR samples

A random poly(ethylene propylene) copolymer containing approximately 4% of ethylene comonomer was used for extrusion of PPR pipes. The melt flow rate was 0.3 dg/min. The ethylene units were distributed randomly along the chains. Chain sequence distribution and tacticity analysis was performed using ^{13}C NMR spectroscopy of 15 wt% PPR solution in 1,1,2,2-$C_2D_2Cl_4$. The spectra were recorded at 120 °C. PPR contained approximately 89 mol% PPP triads, 10 mol% PPE triads and 1 mol% EPE triads. The fraction of isotactic, atactic and syndiotactic PPP triads was approximately 90, 6 and 4%, respectively. The molecular weight of PPR was the following: $M_n = 155 \times 10^3$ g/mol, $M_w = 720 \times 10^3$ g/mol, $M_w/M_n = 4.7$. The material contained additives and pigments, which are typically used for hot water pipes. Pipes of a diameter of 32 mm and a wall thickness of 5.4 mm were extruded at standard conditions ($T_{melt} = 230$ °C) using a single screw extruder.

2.2. Test of PPR pipes under hydrostatic pressure at different temperatures

The hydrostatic pressure resistance of the PPR pipes was performed at Bodycote AB Sweden at different temperatures and pressures. The pressure testing at 20, 50 and 95 °C was performed using deionised water on the inside and on the outside of the specimens. At 110 °C the outside medium was air. The time to failure and the type of failure (brittle, ductile or mixed) were determined by this test. At each condition 3 pipes were tested. Storage conditions and time before breakage of PPR pipes are shown in Table 1. All samples being used in this investigation were taken from the set of pipes of the described pressure testing after they failed.

2.3. Dynamic mechanical thermal analysis (DMTA)

DMTA measurements on typical samples aged at 60 and 110 °C were performed at 1 Hz and at a heating rate of 3 K/min using a Rheometrics RSA.

2.4. DSC

The first melting curve of the broken pipes was measured on a Perkin Elmer DSC 7 at a heating rate of 10 K/min. DSC traces showed a wide temperature range of melting. Melting started at temperatures well below the main melting peak. The temperature of the onset of melting was determined by using the tangential method as shown in Fig. 1. The reproducibility of the melting onset analysis was ±2 °C.

The DSC method was also used for determining the so-called oxidation induction time. The material for this analysis was kept at 200 °C for 10 min under nitrogen atmosphere. The nitrogen was then replaced by oxygen. After a certain time the material started to degrade, which caused a heat flow recorded by DSC. The time for the onset of this heat flow is called oxidation induction time (OIT) and its value depends on the type and the amount of stabilizers.

2.5. Determination of crystallinity by WAXD

A Philips diffractometer using the so-called Braggs–Brentano geometry (reflection) was employed covering an angular range 2θ from 5 to 60° with a step size of 0.005°.

Table 1
Storage conditions and time before breakage of PPR pipes

	Temperature (°C)	Pressure (MPa)	Time before breakage	
			Hours	Days
1	50	9.14	1032	43
2	50	9.29	3715	155
3	50	7.79	8305	346
4	50	7.51	16,153	673
5	70	6.01	2555	106
6	70	5.14	8281	345
7	70	4.80	14,600	608
8	95	5.10	425	18
9	95	3.64	3781	158
10	95	3.01	9743	406
11	95	2.80	13,740	573
12	110	3.93	338	14
13	110	2.82	2532	106
14	110	2.10	10,777	449
15	110	1.71	15,289	637

The degree of crystallinity was determined by employing either the Herman–Weidinger approach or the Ruland approach with the latter taking into account imperfections in the crystals.

2.6. Proton solid-state NMR transverse (T_2) magnetization relaxation

Proton NMR relaxation experiments were performed on a Bruker Minispec NMS-120 spectrometer. This spectrometer operates at a proton resonance frequency of 20 MHz. The length of the 90° pulse and the dead time were 2.8 and 7 μs, respectively. A BVT-3000 temperature controller was used for temperature regulation. The temperature within sample volume was determined with accuracy better than 1 °C.

Three different pulse sequences were used to record the decay of the transverse magnetization (T_2 decay) from both rigid and soft fractions of the samples.

2.6.1. A solid echo pulse sequence (SEPS)

$90°_x - t_{se} - 90°_y - t_{se}$—[acquisition of the amplitude of the transverse magnetization $A(t)$], with $t_{se} = 10$ μs was used to measure the free induction decay. The point in time from the beginning of the first pulse $t = 2t_{se} + t_{90}$ was taken as zero, where t_{90} was the duration of the 90° pulse.

It should be noted that the rigid/soft ratio measured with the SEPS can suffer from systematic errors because of: (1) the incomplete refocusing of the dipolar interactions by the solid-echo for a dipolar network [1]; (2) molecular motions, the correlation time of which is comparable to the pulse spacing [2]; and (3) the shift of the echo maximum due to non-zero pulse width [3,4]. In order to estimate this systematic error, the SEPS experiment was performed at different t_{se}. It can be seen from Fig. 2 that the initial amplitude of the fast decaying component (A^f) decreases significantly with increasing t_{se} contrary to that for slowly decaying component (A^s). Thus, the fraction of A^f is largely underestimated in the SEPS, which does not allow using this experiment for quantitative analysis of the phase composition, if the experiment is performed for one value of t_{se}. Extrapolation of the dependence A^f and A^s on t_{se} to time t_{se} = zero provides the absolute value of the amount of the rigid phase, as determined by a value of $A^f/(A^f + A^s)$. The extrapolated value coincides with that determined by a least squares fit of the free induction decay (FID) after 90° pulse excitation (see Fig. 2). The procedure above requires performing the SEPS experiment for a number of t_{se} values. Analysis of the solid-echo decays has shown that the shape of the fast decaying component approached the Gaussian shape upon decreasing t_{se} in the SEPS. Therefore, the initial part of the FID, as measured with 90° pulse excitation, was fitted with a Gaussian function. Finally, the 90° pulse excitation was used to record FID for the quantitative determination of the rigid phase content.

2.6.2. A Hahn echo pulse sequence (HEPS)

$90°_x - t_{He} - 180°_x - t_{He}$—[acquisition $A(t)$ of the amplitude of an echo maximum], was used to record the slow part of the T_2 relaxation decay for the mobile fraction of the samples, where t_{He} was varied between 35 μs–400 ms. At $t_{He} > 35$ μs, the major part of the signal from the rigid fraction decays nearly to zero. Therefore, the second pulse in the HEPS reverses nuclear spins of the soft fraction only, and an echo signal is formed with a maximum at time $t = 2t_{He} + t_{180}/2$ after the first pulse, where $t_{180}/2$ is the half time of the 180° pulse. By varying the pulse spacing in the HEPS, the amplitude of the transverse magnetization $A(t)$ is measured as a function of time t. The HEPS makes it possible to eliminate the magnetic field and chemical shift inhomogeneities, and to measure the T_2 relaxation time for soft materials/phases accurately.

Thus, both 90° pulse excitation and the HEPS experiments have to be used for an accurate study of both the low

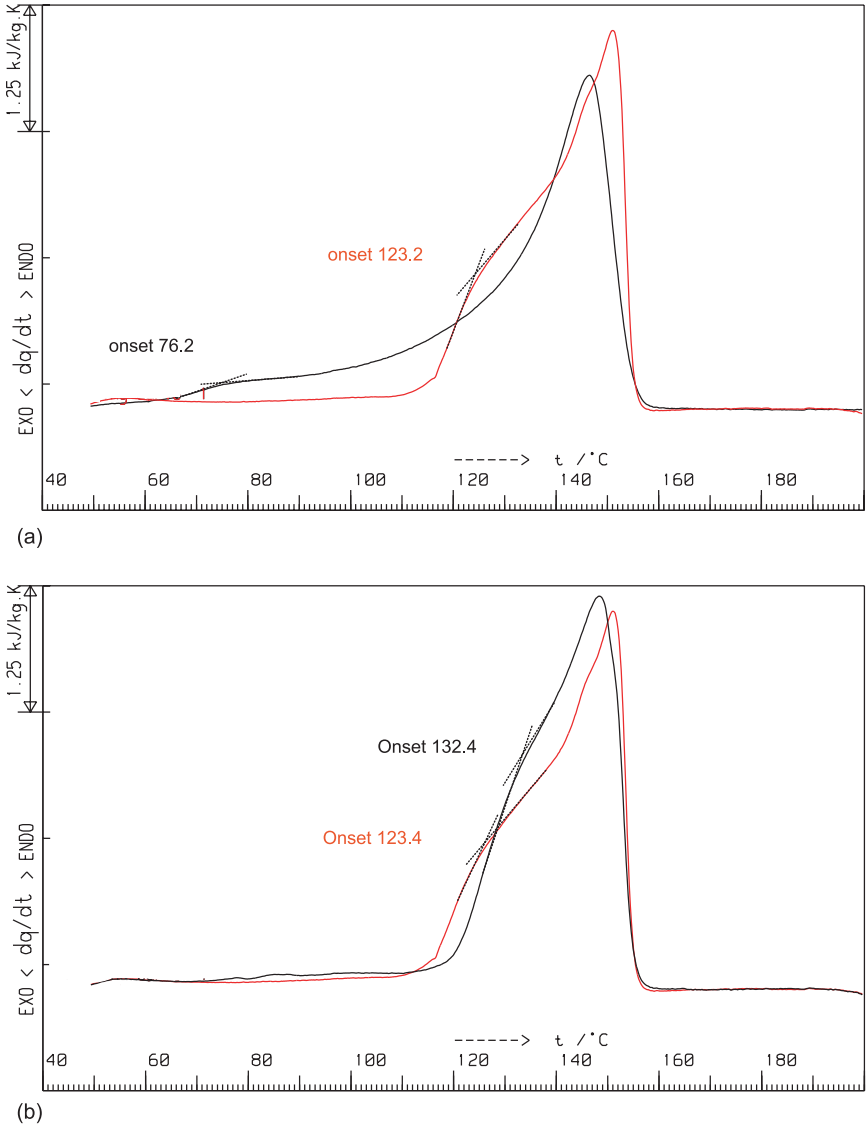

Fig. 1. DSC traces of PPR samples stored under hydrostatic pressure at 50 °C (black line) and 110 °C (red line) for 43 and 14 days, respectively (a); at 110 °C for 14 (red line) and 637 (black line) days (b). The onset of melting is shown on the plots.

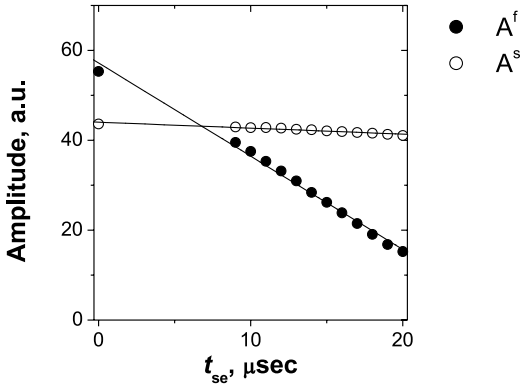

Fig. 2. The initial amplitude of the fast (A^f) and slowly (A^s) decaying components of the transverse magnetization decay against the pulse spacing t_{se} in the SEPS. The amplitudes at $t_{se}=0$ are determined from a least squares analysis of FID measured after 90° pulse excitation. The NMR experiments are performed for a PPR sample at 110 °C.

mobile and the mobile fractions in heterogeneous polymers. The FID recorded after 90° pulse excitation is used to determine the relaxation time and the amount of the rigid material. The HEPS is used to determine the relaxation behaviour for the soft material. The recording of the FID and the HEPS lasted for approximately 6 min and 2.5 h, respectively.

The FIDs, as recorded after 90 °C pulse excitation, were fitted with a linear combination of Gaussian and exponential functions:

$$A(t) = A(0)^c \exp[-(t/T_2^c)^2] + A(0)^l \exp[-t/T_2^l], \quad (1)$$

Only the initial part of the decay ($0=\tau<100$ µs) was fitted. In this fit, the base line was fixed to the value that was measured at the same conditions for the NMR tube without the sample.

The decay of the transverse magnetization, as measured

with the HEPS, was fitted with a linear combination of three exponentials functions:[1]

$$A(t) = A(0)^{\mathrm{i}} \exp[-t/T_2^{\mathrm{i}}] + A(0)^{\mathrm{a}} \exp[-t/T_2^{\mathrm{a}}] + A(0)^{\mathrm{r}} \exp[-t/T_2^{\mathrm{r}}], \quad (2)$$

Superscripts in Eqs. (1) and (2) stand for 'c' (crystalline phase), 'i' (interface), 'a' (soft amorphous phase) and 'r' (rubbery-like fraction). The time constants (T_2 relaxation time), which are characteristic of different slopes in the magnetization decay curve, are related to molecular mobility. The longer the T_2 relaxation time is, the larger the frequency (and/or the amplitude) of the molecular motions. The relative fraction of the relaxation components, $\{A(0)^{\mathrm{index}}/[A(0)^{\mathrm{c}}+A(0)^{\mathrm{i}}+A(0)^{\mathrm{a}}+A(0)^{\mathrm{r}}]\}\times 100\%$, as designated in the text by $\%T_2^{\mathrm{index}}$, represents the fraction of hydrogen in phases/components with different molecular mobility.

The relative error in the relaxation parameters is composed of (a) experimental errors (about 1%), (b) an error caused by a chosen fitting function (estimated to be about 5%) and (c) uncertainties of the fitting (about 0.5%). Repeated experiments for the same sample indicate that the reproducibility of the relaxation parameters was smaller than 2%.

The recovery of the longitudinal magnetisation (T_1 relaxation) was measured with the inversion-recovery pulse sequence using solid echo pulses for the signal detection, $180°_x - t_{\mathrm{var}} - 90°_x - t_{\mathrm{se}} - 90°_y - t_{\mathrm{se}}$—[acquisition: $A(0)$], with $t_{\mathrm{se}} = 10\ \mu\mathrm{s}$. Inversion-recovery curves were fitted with a linear combination of two exponential function with characteristic time constant T_1^{s} and T_1^{l}:

$$A(t_{\mathrm{var}}) = A(0)^{\mathrm{s}}[1 - 2\exp(-t_{\mathrm{var}}/T_1^{\mathrm{s}})] + A(0)^{\mathrm{l}}[1 - 2\exp(-t_{\mathrm{var}}/T_2^{\mathrm{l}})], \quad (3)$$

where superscripts 's' and 'l' correspond to short and long T_1 relaxation time. The reproducibility of the results was about 5%.

The spin–lattice relaxation in the rotating frame ($T_{1\rho}$) was measured with the spin-locking after 90° pulse [5]. The data were analyzed with a linear combination of three exponential functions. The radio-frequency field strength of 8.15 kHz was used in this experiment.

The recycling delay time for all NMR experiments was longer than $5T_1^l$.

3. Results and discussions

3.1. Fracture behaviour of PPR pipes exposed to hydrostatic pressure

The results of the hydrostatic pressure tests are shown in Fig. 3. According to our expectations the pipes broke either due to ductile failure under higher pressures and shorter times or due brittle failure at lower pressures and longer times. This behaviour can be explained due to different failure mechanisms. In the first case (at the short storage time), the failure is mainly determined by material damage caused by the mechanical load and it is therefore related to the overall stiffness of the material, as determined by E-modulus and yield stress. At certain pressures, the material starts to yield, which is followed by ductile failure. At longer times after the change in the slope of lines in Fig. 3, the dependence of failure stress on time becomes more pronounced. The material breaks due to brittle failure because of ageing effects and mechanical load. The explanation of this brittle failure is as follows. Small crazes are being formed around rigid inclusions, such as pigments, additives and catalyst residues. Craze formation facilitates diffusion of air into the material. Therefore, stretched chains in the fibrillar structures are more easily accessible to oxygen in air. Moreover, the thermal oxidation of highly stretched chains is favoured due to local forces causing main-chain bond deformation.

The additive package, i.e. combination and amount of additives, has an influence on the occurrence of this failure mechanism, because the stabilizers can prolong the lifetime of a pipe by slowing down the failure of crazes due to thermal oxidation. As can be seen in Fig. 3, the temperature affects the failure time significantly. In order to prolong the lifetime of PPR pipes to approximately 50 years, it is necessary to limit the usage temperature and the usage time of pipes at higher temperatures.

3.2. Additives analysis and thermal oxidation of PPR pipes

Since stabilizers are consumed upon thermal oxidation, oxidation induction time (OIT) and an oven-ageing test can possibly be used for determining storage time. The oven-ageing test was performed at 140 °C and air atmosphere. In this test, time for visual changes in surface roughness and

[1] The decay of the transverse magnetization (T_2 decay) is caused by different mechanisms for rigid solids and highly mobile molecules. In rigid solids, the decrease of the transverse magnetization after an excitation does not require molecular motions and is caused by dipolar dephasing (coherent process). The T_2 relaxation of highly mobile molecules is due to stochastic modulations of local fields by molecular motions (incoherent process). Coherent and incoherent processes determine the T_2 relaxation for the intermediate motional regime. The description of the decay of the transverse magnetization for heterogeneous polymers is very complex because of the following reasons: (1) soft polymeric materials and soft phases in heterogeneous polymers reveal both the solid-like (slow, long spatial scale) and liquid-like (fast, local) chain motions that results in complex shape of the T_2 relaxation decay; (2) a morphological heterogeneity of polymeric materials resulting in a wide frequency distribution of molecular motions. Therefore, the theoretical description of the shape of the T_2 decay for two-phase polymers above T_g is still under debate and purely phenomenological description of the decay shape with two- or more components is commonly used.

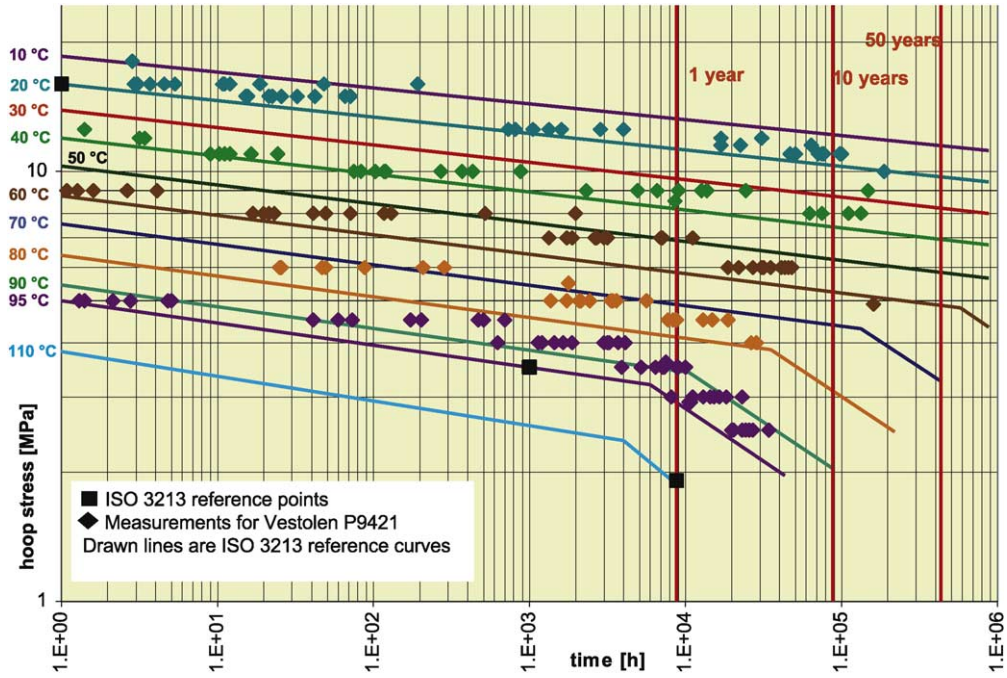

Fig. 3. Results of the hydrostatic pressure tests showing circumferential stress (hoop stress) against storage time of PPR pipes at different temperatures. The shown points are results of the measurements where colours of data points correspond to the testing temperature that is indicated with the same colour on the left side of the Figure. Drawn lines of the same colour are references, which show the minimum stress level at a certain storage time and temperature according to ISO 3213:1996(E) International Standard 'Polypropylene (PP) pipes—effect of time and temperature on the expected strength'. All measurement points have to lie on/or above those lines to fulfil the requirement for usage of a certain PPR grade in pipes. The time of abrupt change in the slope of lines that is visible above 60 °C corresponds to a change in failure mechanism from ductile to brittle. Black squares correspond to required stresses measured at certain testing temperatures and times for the approval of a new polymer grade in the market.

cracks formation was determined. Material history cannot be distinguished properly using this test. The influence of storage time and temperature on the OIT is shown in Fig. 4. The OIT decreases with increasing storage time and temperature. However, the OIT value is hardly influenced by storage time after pipes are stored above 80 °C for longer than 1 year. Therefore, this method cannot be used for determining the long storage time.

Another method, which was used for determining the amount of remaining long-term stabilizers, was high-pressure liquid chromatography (HPLC). The results of this method are comparable with those of OIT measurements, i.e. no significant changes are observed in the amount of stabilizers after one-year storage time above 80 °C.

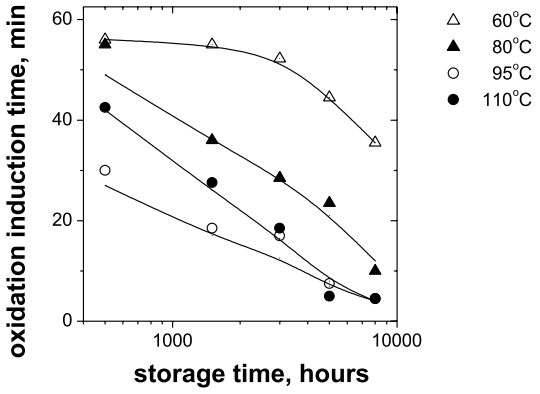

Fig. 4. The effect of storage time at different temperatures on oxidation induction time (OIT). Samples for OIT study were taken after the same hydrostatic pressure tests as those studied by NMR.

Long-lasting exposure of PPR to elevated temperatures can result in chain scission and/or crosslinking that could affect failure behaviour of PPR pipes. In order to determine possible changes in the molecular structure of PPR chains, viscosity of PPR solutions in decaline was measured at 135 °C. Viscosity is almost the same for all studied samples both for inner and outer parts of PPR pipes, which exclude possible effects of chain degradation on failure behaviour. Therefore, physical ageing should be the origin of pipe breakage.

3.3. DMTA measurements and linear expansion coefficient

DMTA measurements and the linear expansion coefficient (CLTE) are used to determine possible changes in the physical structures upon ageing. The temperature dependence of the E-modulus and the $\tan\delta$ are shown for 4 representative samples in Fig. 5(a) and (b). The glass transition temperature, T_g, and storage modulus are only slightly affected by storage time and temperature. CLTE measurements are even less sensitive towards changes upon storage conditions. Thus, these two methods do not lead to

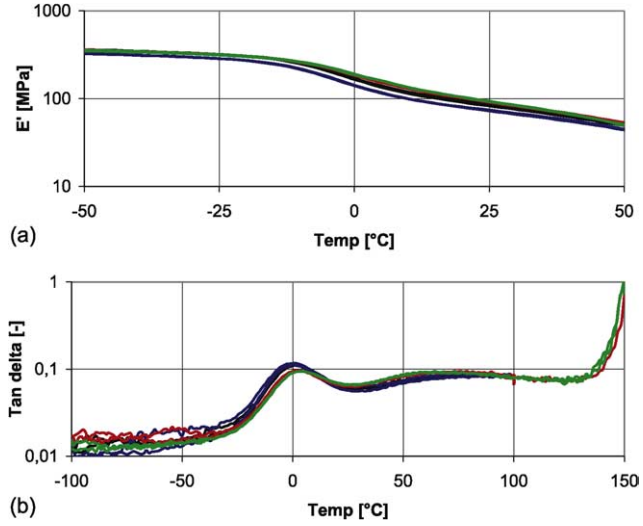

Fig. 5. DMTA data: storage modulus E' (a) and tangent delta (b) for PPR pipes stored for different time at different temperatures, as shown by lines of different colours: black—21 days at 110 °C; blue—573 days at 110 °C; red—21 days at 60 °C; green—without thermal treatment.

any measurable difference between long and short storage time.

3.4. Crystallinity as determined by WAXD

WAXD is used for determining the effect of ageing time on crystallinity. Two samples with extreme storage conditions are studied: one sample was stored at 50 °C for 43 days and the other one-at 110 °C for 637 days. The crystallinity slightly increases from about 40 to 42% upon increasing temperature and storage time. The crystallinity is the same both for inner part and skin layer of the pipes. Mainly, α-crystal polymorph is present in the skin layer. A small amount of γ-crystals is detected in the core part of the pipes. Thus, overall crystallinity and ratio of α-, γ- crystals are not sensitive to storage time and temperature.

3.5. Changes in melting behaviour upon storage

It is well established that annealing of semicrystalline polymers causes significant changes in melting behaviour due to an increase in crystallinity and changes in morphology [6]. DSC traces of all stored pipes show that melting starts at temperatures well below the main melting peak (Fig. 1). The temperature of melting onset is determined as temperature at which a change of the slope of the dependence of heat flow on temperature is observed, as shown in Fig. 1. Annealing of samples causes a shift of melting onset temperature towards higher temperatures. The maximum storage temperature of a damaged pipe or fitting can be calculated from the onset temperature using the following relationship: $T_{onset} = (0.87T_{exposure}) + 32.8$; (see Fig. 6) [7]. However, the storage time cannot be determined with high accuracy, since the onset temperature does not

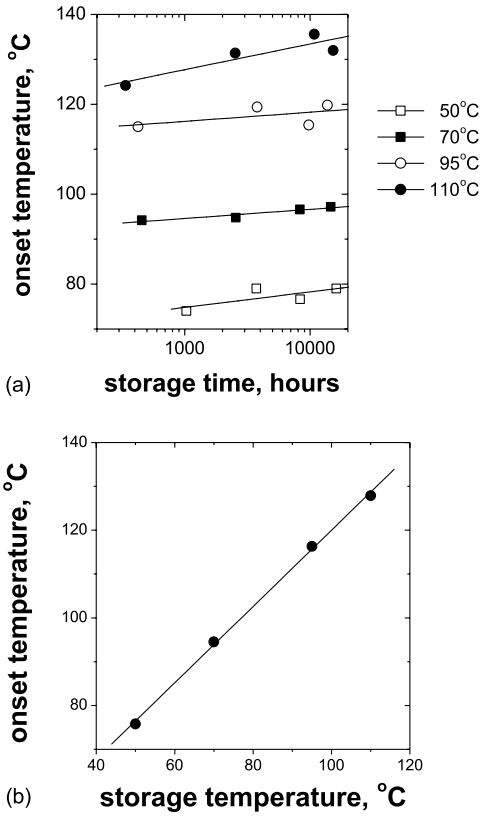

Fig. 6. (a) Onset temperature of melting of PP crystals against storage time of PPR pipes under hydrostatic pressure at different temperatures, as shown on Figure insert. The lines represent the result of a linear regression analysis. (b) Onset temperature of melting of PPR pipes stored under hydrostatic pressure for 42 days against storage temperature. The onset temperature is determined by a least squares analysis of the data in (a). The line represents the result of a linear regression analysis: intercept = 32.8 ± 1.8 °C; slope = 0.87 ± 0.02. The correlation coefficient equals 0.983.

change significantly with the storage time (see Fig. 6(a)). Since a short-time use of pipes and fittings at higher temperatures is acceptable, it is important to determine not only usage temperature but also the storage time.

3.6. Molecular mobility and phase composition of samples as studied by ^1H solid-state NMR magnetization relaxation

All the methods that were applied above suffer from a lack of sensitivity to changes caused by storage time. In the following, solid state NMR will be described as the only method that is able to detect the small differences in the polymer morphology that occur during such a long storage under hydrostatic pressure.

3.6.1. A change in the lamellae thickness by spin–lattice (T_1) relaxation analysis

Analysis of proton spin–lattice (T_1) relaxation can be used to estimate lamellae thickness in semicrystalline polymers or the shortest distance across domains in the case of more complex morphologies [8–10]. T_1 relaxation of heterogeneous materials is largely affected by

spin-diffusion, i.e. a spatial transfer of the nuclear magnetisation between phases by mutual spin flips via the strong dipole–dipole interactions among nuclear spins [11]. If the size of regions with different molecular mobility is below about a few nanometers, the magnetisation transfer is very efficient causing a single T_1 relaxation. An increase in domain size reduces the effect of the spin-diffusion and causes a multi-component relaxation. In the case of semicrystalline polymers, the relaxation components with the longest (T_1^l) and shortest (T_1^s) relaxation time are primarily associated with the crystalline and the amorphous phases, respectively. It has been shown that T_1^l for high density PE is proportional to the square of the lamellae thickness [8].

^{1}H T_1 relaxation of PPR samples can be described with two components. The relative fraction of these components is hardly affected by storage time under hydrostatic pressure, whereas T_1^l and T_1^s slightly increase with increasing storage time (Fig. 7). This increase in the T_1 values can be caused by the following reasons: (1) increasing crystallinity, (2) changes in molecular mobility in both phases, and (3) increase in the lamellae thickness. Although crystallinity, as determined by solid-state NMR, slightly increases with increasing storage time, this increase cannot cause observed changes in the T_1 values due to the following fact. T_1^l is approximately the same for all samples with the same storage time, whereas crystallinity of samples with the same storage time increases with increasing storage temperature, as will be shown below. Molecular mobility in different phases is not largely affected by storage time, as it follows from $T_{1\rho}$ and T_2 relaxation experiments, which will be discussed below, and from minor change in T_g upon storage time. Therefore, a slight increase in T_1^l with increasing storage time might be caused by 1–2% increase in the lamellae thickness and/or perfection of crystals.

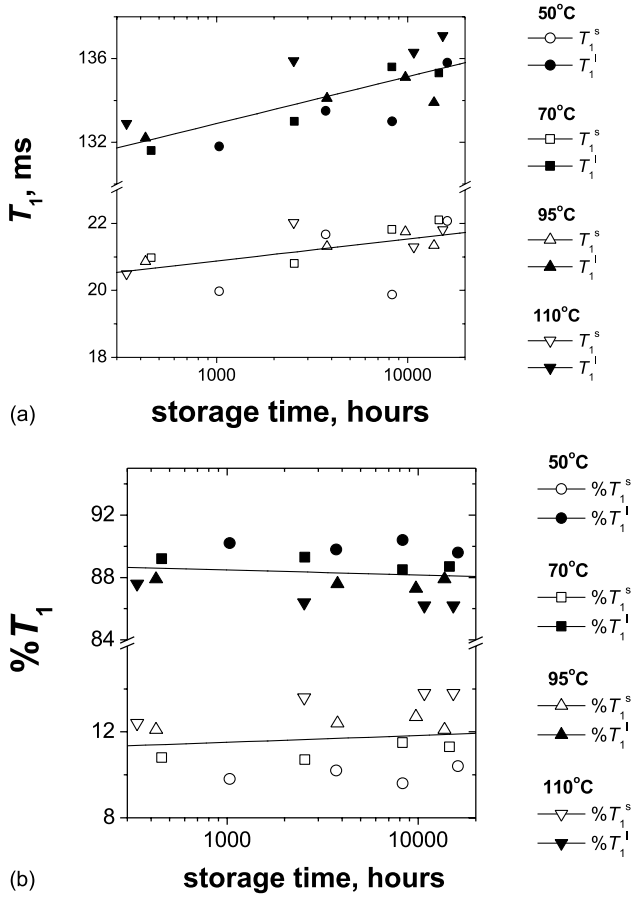

Fig. 7. ^{1}H T_1 relaxation times (a) and the fraction of the T_1 relaxation components (b) against storage time of PPR pipes under hydrostatic pressure at different temperatures, as shown in Figure insert. The NMR relaxation parameters were measured at 50 °C. The lines represent the result of a linear regression analysis.

3.6.2. Analysis of microphase structure and molecular motions by proton T_1, $T_{1\rho}$ and T_2 NMR magnetization relaxation

Microphase structure, morphology and molecular motions in PP were extensively studied by solid state, proton NMR transverse magnetization (T_2) relaxation [12–21]. It was shown that the sensitivity of NMR to thermal ageing of isotactic PP exceeds that of DSC [21]. These NMR studies have shown that the method provides information about the phase composition and molecular mobility in different phases of PP. In general, a three-phase model is suggested from the results of these experiments, namely a crystalline phase, a semi-rigid crystal–amorphous interphase and a soft fraction of an amorphous phase can be studied with this method. 'Modeling the morphology as a two-phase system, i.e. crystalline (CR) and non-crystalline (NC), is an oversimplification. Indeed there is an interface, and it is ludicrous to assume that chains should go from fully ordered (CR) to disordered (NC) without a finite region where this transition is made' [21]. Distinct differences in chain mobility in the different phases of PP are apparently caused by a short statistical segment of PP chain, which is about 6 carbon–carbon backbone bonds [22–24]. This results in a fast loss of restrictions on rotational and translational chain mobility when moving away from the crystalline phase. It is noted that the fraction of the intermediate phase depends on the technique, temperature and the method for the data evaluation. In many respects, the intermediate phase has a kinetic origin and may not be considered as a true thermodynamical phase. Apparently, the definition of an interface or a semi-rigid fraction of the amorphous phase is more appropriate for the third phase.

The length of tie molecules between adjacent crystals and the chain confinement exerted on the amorphous phase by crystallites largely affect the T_2 relaxation of the soft amorphous phase at temperatures well above T_g [18,25,26]. Therefore, NMR sensitivity to crystallinity and morphology is considerably enhanced by analysing the T_2 relaxation time of the amorphous phase [18]. It was also shown that the NMR method is very sensitive to changes in crystallinity and strain induced chain orientation in PP samples upon uniaxial stretching, stress relaxation and annealing [27–30].

Molecular motions in polymer materials can be studied

in a wide frequency range by means of various proton NMR relaxation experiments [31]. The spin-lattice (T_1) relaxation data provide information about fast (in the range of tens–hundreds MHz) local motions. The spin-lattice relaxation in the rotating frame ($T_{1\rho}$) allows measuring slower molecular motions with the frequency of about tens of kHz. ^{1}H T_1 and $T_{1\rho}$ relaxation parameters for studied PPR samples show hardly any change upon storage time at different temperatures. The T_2 relaxation above T_g is mainly determined by slow, large spatial scale chain mobility. Therefore, this relaxation process is the most sensitive tool for analysis of chain mobility in soft materials and soft phases in polymers [32]. Moreover, the results of proton T_2 relaxation experiments for heterogeneous materials are easier to interpret than those of T_1 and $T_{1\rho}$, because ^{1}H T_2 data are not complicated by the effect of spin-diffusion [31]. Therefore, changes in the phase composition and molecular mobility upon storage of PPR pipes at different temperatures are analysed below by ^{1}H T_2 relaxation analysis.

3.6.3. Molecular mobility and phase composition by proton transverse magnetization relaxation

The T_2 relaxation experiments for PPR as a function of temperature have shown that these experiments provide the largest distinction in the relaxation behaviour of different phases at measurement temperatures above 100 °C. All NMR experiments were performed at 110 °C because this temperature is significantly lower then the melting temperature of the PPR crystalline phase, as was shown by DSC: the melting peak for all samples is observed at about 150 ± 2 °C; the onset of melting for samples stored at 50 and 70 °C is observed below 110 °C (see Figs. 1 and 6). In order to check a possible effect of sample annealing during the NMR experiment at 110 °C, the experiment was repeated at the same temperature and conditions for one of the samples. These experiments show that crystallinity hardly changes even after 2 h (the time required for measuring T_2 relaxation parameters) at 110 °C.

The T_2 relaxation decay for PPR samples consists of four distinct components (see Fig. 8). The characteristic decay times of these components is in the range typical for the following material/phases (Fig. 9):

(1) Crystalline phase and rigid fraction of the crystal–amorphous interface—($T_2^c \approx 0.016$ ms).
(2) Semi-rigid crystal-amorphous interface—($T_2^i \approx 0.1$ ms).
(3) Soft fraction of the amorphous phase—($T_2^a \approx 0.6$ ms).
(4) Highly mobile rubbery-like material—($T_2^r \approx 2.5$ ms).

The characteristic decay time, T_2^{index}, is related to molecular mobility, which is closely related to hardness/-softness of different fractions of PPR. Shorter T_2 relaxation time corresponds to larger modulus. The relative intensity of the relaxation components, $\%T_2^{index}$, corresponds to weight

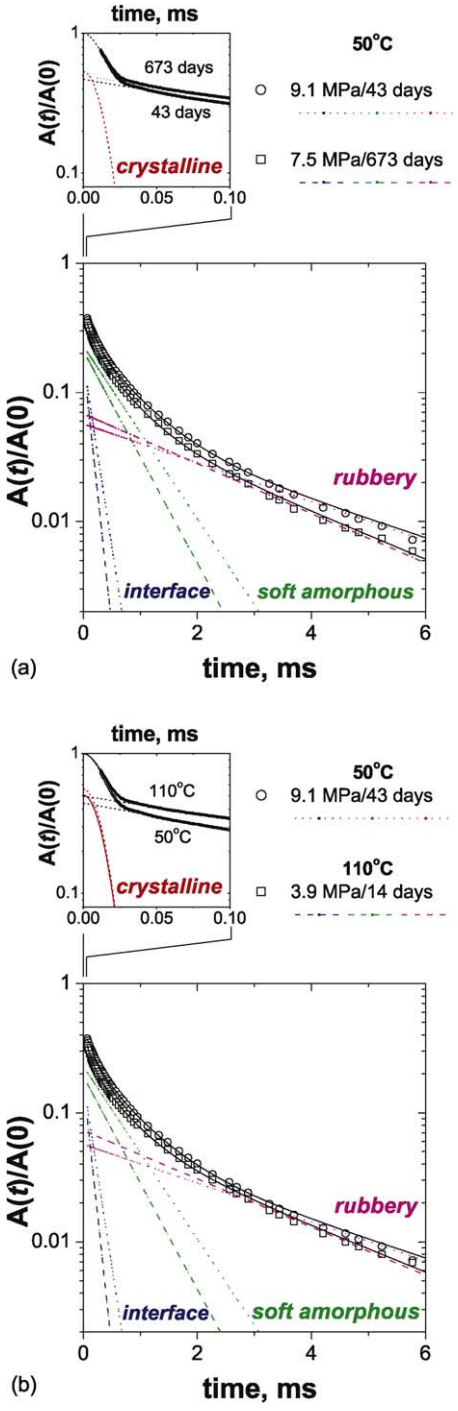

Fig. 8. The T_2 relaxation decay for PPR samples stored under hydrostatic pressure at 50 °C for 43 and 673 days (a), and for PPR samples stored under hydrostatic pressure at 50 and 100 °C for 43 and 14 days, respectively (b). The decay was measured at 110 °C. The upper insert shows FID of the same samples measured after 90° pulse excitation. The T_2 relaxation decay for the soft fractions of PPR, as measured with the HEPS, is shown below. The amplitude of the transverse magnetisation, $A(t)$, for both experiments was normalized to its value at time zero, $A(0)$. $A(0)$ value was determined by a least squares fit of the FID recorded after 90° pulse excitation. The solid line represents the result of a least squares adjustment of the FID with a linear combination of Gaussian and exponential functions. Dotted and dashed lines show separate components.

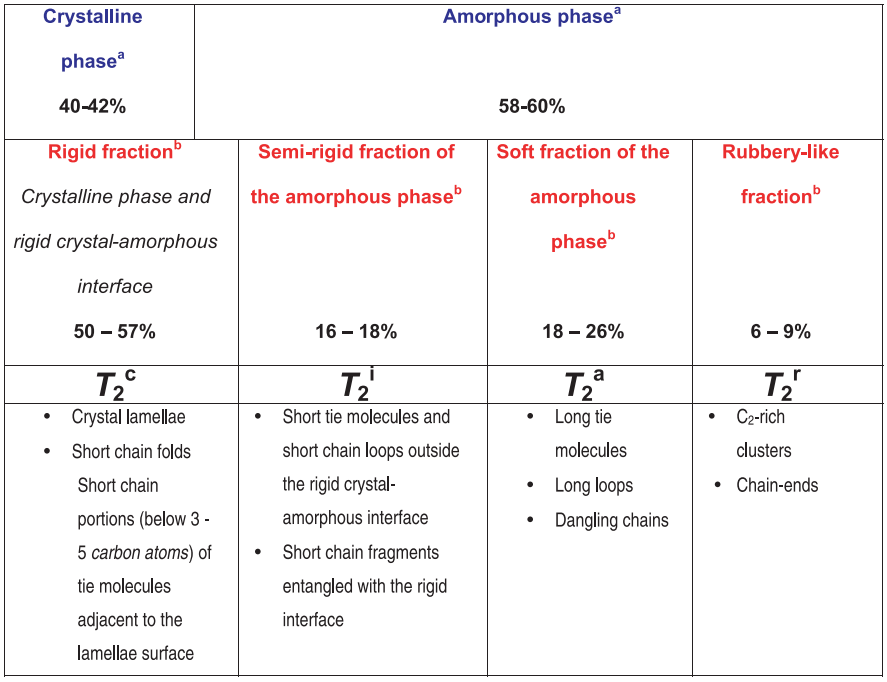

Fig. 9. Schematic drawing of the phase composition of PPR and morphological structures in the relation to T_2 relaxation components.

percent of PPR fractions/phases revealing different molecular mobility.

This assignment of the T_2^c, T_2^i and T_2^a relaxation components is based on previous solid-state NMR studies of PP [12–20]. As far as the T_2^r relaxation is concerned, we suggest that this relaxation component originates from nano-clusters of rubbery-like material whose composition is largely enhanced by ethylene chain units, and possibly atactic chain units of PP-rich chain fragments. This assignment is supported by the following facts. (1) It is well established that ethylen–propylen rubber is well phase separated from i-PP in blends of these polymers [33,34]. (2) ^{13}C NMR studies of ethylene–propylene rubbers has shown that the comonomer units cannot be present throughout the interface between the crystalline PP and the amorphous phase. The comonomer units are mainly present at the more mobile core part of the amorphous phase [21,35]. (3) An increase in the atactic fraction has essential effect on ^{1}H T_2 relaxation of PP, i.e. the relative intensity of the relaxation component with the longest decay time increases with increasing the amount of atactic fraction [36,37]. This allows a use of low-field NMR for fast tacticity analysis on production cites. (4) The relative intensity of T_2^r relaxation component, $\%T_2^r$, is slightly larger than the total amount of ethylene containing triads of PPR. (5) A value of T_2^r at 110 °C is in the range that is typical for non-vulcanized EPDM rubber [38], and T_2^r is much longer than T_2 for a soft fraction of the amorphous phase of PP homopolymer at 110 °C [13–16,19]. This large difference in T_2 values is due to much lower T_g of EPDM than that of PP homopolymer.

The rigid fraction of PPR ($\%T_2^c$), as measured by the NMR method at 110 °C, can be used as a measure of crystallinity. In general, different methods for crystallinity determination do not always yield the same results on exactly the same sample [39] because of the following reasons: (a) complex morphology of semicrystalline polymers requiring different sets of assumptions for the analysis of data recorded by the different techniques; (b) the two-phase model is rather simplified for describing semicrystalline polymers due to the presence of a crystal-amorphous interface, which can be detected either as crystalline or amorphous fraction depending on the method used [39]; (c) discrimination of the crystalline phase from the amorphous one is made on a basis of different characteristics, such as the enthalpy of melting (DSC), long range periodicity (WAXD), bond vibrations (vibrational spectroscopy), the specific volume (density analysis) and molecular mobility (NMR). For example, WAXD determines only large crystals consisting of several crystal unit cells, whereas NMR crystallinity includes both large and small nano-size crystals, and crystals with a large fraction of defects [40–42]. Therefore, the NMR crystallinity for PPR samples is larger than its value determined by WAXD, i.e. 50–57% and 40–42%, respectively.

The effect of storage time and temperature on the T_2

relaxation parameters of PPR is shown in Figs. 10 and 11. Molecular mobility in the crystal-amorphous interface, the soft amorphous phase and the rubbery-like material slightly decreases upon storage time under hydrostatic pressure (Fig. 10). The NMR crystallinity, as determined by $\%T_2^c$, increases with increasing storage temperature, as can be seen in Fig. 11(a). The growth in crystallinity is the largest during first two weeks storage at 95 and 110 °C, as compared with pipes stored at 50 and 70 °C. At longer storage time, crystallinity increases by 1–2% at all temperatures. Storage of samples under hydrostatic pressure causes also significant changes in the amorphous phase. The fraction of semi-rigid ($\%T_2^i$) and soft amorphous ($\%T_2^a$) phases slightly decreases upon storage at the expense of the rubbery-like fraction ($\%T_2^r$), as can be seen in Fig. 11(b)–(d).

Since the molar mass of PPR does not change upon long-time annealing, the following physical processes, which occur in PPR due to exposure to hydrostatic pressure at elevated temperatures, can cause the changes in the phase composition:

(1) Creep upon hydrostatic pressure causing chain elongation in the amorphous phase. It was shown previously that uniaxial stretching of PP causes significant immobilization of the amorphous phase [30].
(2) Annealing of samples during storage that causes a few percent increase in the crystallinity. This increase in crystallinity can occur due to the attachment of chain fragments in the amorphous phase to existing crystals and/or due to formation of new crystals. In both cases, mobility in the amorphous phase decreases due to a decrease in the chain length between adjacent crystals, i.e. the length of tie molecules.
(3) It is suggested that annealing causes an increase in the gradient of concentration of ethylene-rich chain fragments through the mobile fractions of the amorphous phase. This suggestion is supported by the following results obtained in previous studies of i-PP: (i) the increase in the rigid fraction of PPR upon annealing is caused by build up of PP stems on the faces of existing crystallites and/or formation of new small, crystalline entities, such as fringed micelles [21]. (ii) The interface is mainly formed by PP chain fragments [21]. (iii) The concentration of ethylene chain units increases towards inner, more mobile parts of the amorphous phase [35]. Since the ageing of PPR samples causes a few percent increase in the amount of rigid phase (Fig. 11(a)) and a slight increase in the amount of interface (Fig. 11(b)), this results in an enrichment of the mobile fractions of the samples by ethylene chain units. Since ethylene containing chain fragments tends to be phase separated from the PP matrix [21,35], this can cause a slight increase in the fraction of rubbery-like material ($\%T_2^r$) (Fig. 11(d)). The phenomena above would favour a larger gradient of concentration of ethylene-rich chain fragments through the mobile fractions of the amorphous phase. The better phase separation results in an additional decrease in molecular mobility in the PPR matrix, since more mobile ethylene chain units, if they are molecularly mixed with the PP matrix, cause some increase in molecular mobility of the matrix material due to intermolecular coupling of chain motions.

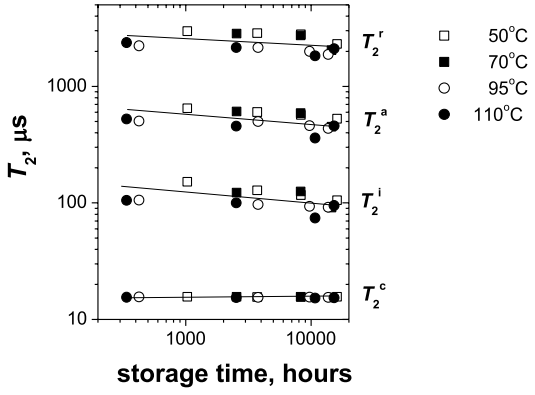

Fig. 10. The ^{1}H T_2 relaxation time for different phases against storage time of PPR pipes under hydrostatic pressure at different temperatures, as shown on Figure insert. The relaxation times T_2^c, T_2^i, T_2^a and T_2^r correspond to the relaxation of crystalline phase and rigid fraction of crystal-amorphous interface (T_2^c), semi-rigid crystal-amorphous interface (T_2^i), soft fraction of the amorphous phase (T_2^a) and rubbery-like material (T_2^r). The lines represent the result of a linear regression analysis. The relaxation parameters were measured at 110 °C.

The overall immobilization of the amorphous phase upon storage time is the most clearly seen from comparison of the relaxation rate of the amorphous phase as a whole, $\sum_{i,a,r}(fT_2^{-1})$, which is defined as $a[\%T_2^i/T_2^i + \%T_2^a/T_2^a + \%T_2^r/T_2^r]$, where $(\%T_2^i + \%T_2^a + \%T_2^r) = 1$ (see Fig. 12). The shorter the overall relaxation rate, the more rigid the amorphous phase is. Immobilization of the amorphous phase upon storage at 50 and 70 °C is significantly smaller than that at 90 and 110 °C. It can be seen that already relatively short storage times above 90 °C causes significant immobilization of the amorphous phase as a whole. Since the molar mass of PPR does not change upon long-time annealing even at 110 °C, no decrease in the number of tie molecules interconnecting crystallites occurs. Therefore, breakage of PPR pipes is mainly caused by an increase in the amount of rigid fraction and rigidity of the amorphous phase, which cause embrittlement of PPR pipes followed by a failure.

Thus, combined use of DSC and proton NMR T_2 relaxation experiments allow estimating both time and temperature of storage of PPR pipes under hydrostatic pressure and elevated temperatures. DSC experiments allow determining the maximum storage temperature from the increase in temperature of the melting onset. Immobilisation of the amorphous phase and an increase in the amount of rigid fraction, as measured by solid-state NMR T_2 relaxation, can be used for determining storage time using unaged samples as a reference.

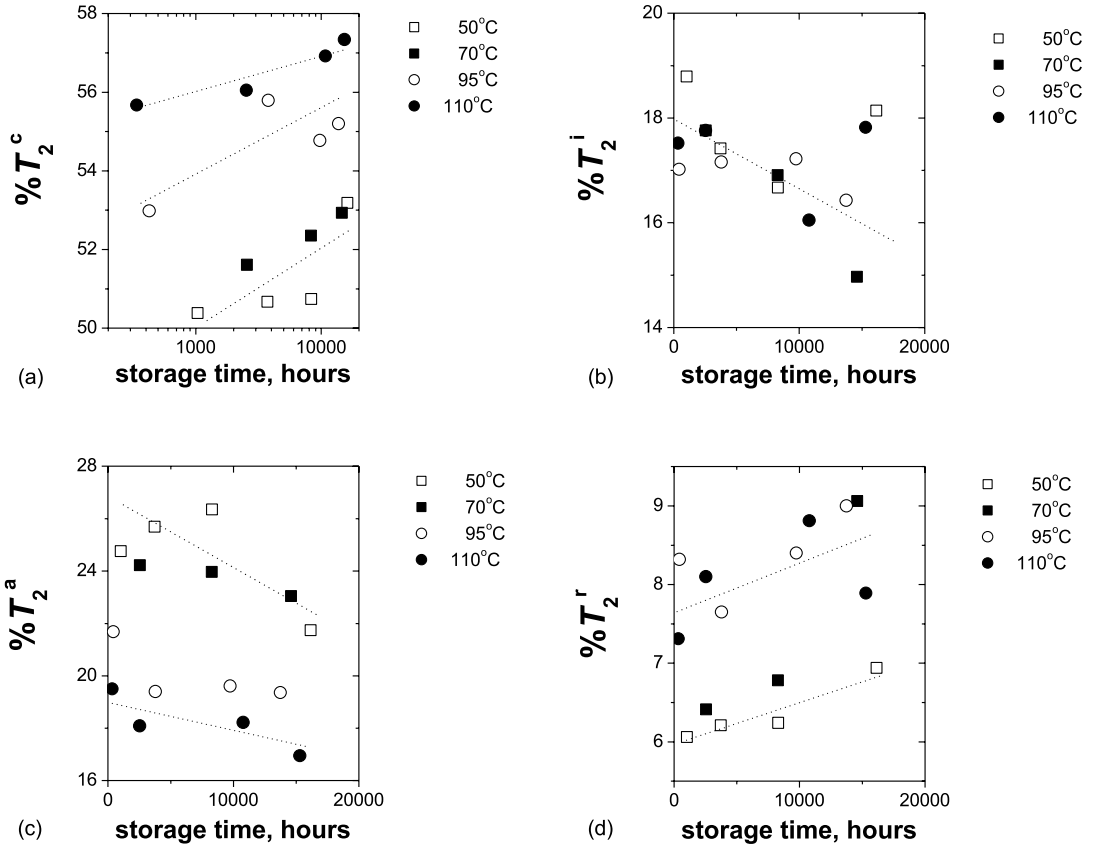

Fig. 11. The effect of storage time of PPR pipes under hydrostatic pressure at different temperatures on the phase composition. Storage temperature is shown on Figure insert. Lines are guide for the eye. (a) The fraction of crystalline phase and rigid fraction of crystal–amorphous interface; (b) the fraction of semi-rigid crystal–amorphous interface; (c) the soft fraction of the amorphous phase; (d) the fraction of rubbery-like material. The phase composition was measured at 110 °C.

4. Conclusions

Changes in chemical and physical structures of PPR pipes upon storage at different times and temperatures under hydrostatic pressure have been studied with a number of techniques. It was shown that techniques, that are sensitive to thermooxidative degradation of PPR, like the OIT, viscosimetry and consumption of stabilizers measured by HPLC, cannot be used for determining storage times longer than 1 year. Since the molar mass of PPR does not change upon long-time annealing even at 110 °C, breakage of PPR pipes is mainly caused by changes in physical structures. Several methods were used in the present study for analysis of physical structures in PPR. Crystallinity of the samples, as determined by WAXD, was not largely affected by storage time and temperature. The modulus and tan δ of the samples were only affected by storage temperature, which is related to the slight increase in crystallinity. It was shown that usage temperature of PPR pipes or fittings can be determined from the onset temperature of melting from DSC traces. The storage time on the other hand cannot be determined with high accuracy using this method. Thus, all these methods above did not give any clear dependence of measured parameters on storage time.

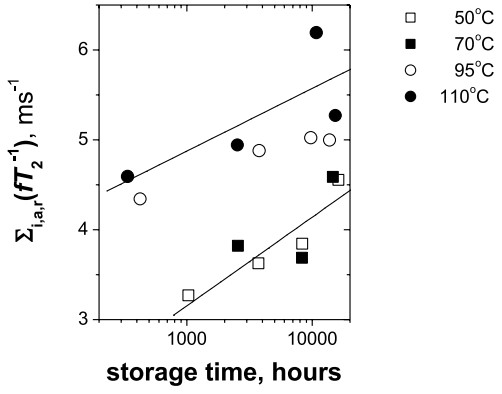

Fig. 12. The relaxation rate of the amorphous fraction as a whole, $\sum_{l,a,r}(fT_2^{-1})$, against storage time of PPR pipes under hydrostatic pressure at different temperatures, as shown on Figure insert. The relaxation rate $\sum_{l,a,r}(fT_2^{-1})$ equals $[\%T_2^i/T_2^i + \%T_2^a/T_2^a + \%T_2^r/T_2^r]$, where $[\%T_2^i + \%T_2^a + \%T_2^r] = 1$. The relaxation rate was measured at 110 °C.

It was shown that proton NMR T_2 relaxation experiments are sensitive to both storage temperature and time. The experiments allow determining the amount of four different fractions of PPR samples, i.e. (1) rigid fraction, which is composed of the crystalline phase and the rigid fraction of the crystal-amorphous interface, (2) semi-rigid

crystal-amorphous interface that is formed by chain units adjacent to the lamellae surface, (3) soft fraction of the amorphous phase, and (4) rubbery-like material, which is enriched by highly mobile ethylene containing chain fragments. These phases are discriminated on the base of a large difference in molecular mobility. The most pronounced changes upon long storage time are observed for the rigid fraction of PPR (fraction 1). Its amount increases from about 50% at short storage time at low temperatures, to 57% at storage at high temperature for times of about 2 years. It is noted that the fraction of the rigid phase is significantly larger compared to WAXD crystallinity, which is about 40 and 42% for samples stored at 50 °C for 43 days and at 110 °C for 637 days, respectively. This difference between the NMR and WAXD data is attributed to the presence of small imperfect crystals as well as rigid crystal-amorphous interface, which are not detected by WAXD and DSC. The increased amount of the rigid amorphous phases imposes additional constraints on molecular mobility in three different fractions of the amorphous phase (fractions 2–4). The following reasons cause the overall decrease in molecular mobility upon long time annealing of the samples at temperatures far above T_g of PPR, which is about 0 °C: (1) perfection of existing crystals and the formation of new crystals, which act as physical junctions leading to immobilization of the amorphous phase, (2) creep under hydrostatic pressure causing chain elongation in the amorphous phase, and (3) a better phase separation of ethylene chain fragments from the PPR matrix. All these changes cause embrittlement of the samples followed by a failure. Thus, the combination of DSC and solid-state NMR relaxation experiments is a powerful tool for the investigation of the molecular origin of damages in broken PPR pipes and fittings and for estimating their usage temperature and time.

Acknowledgements

The authors would like to thank Jan Smeets for recording and evaluating DSC data, Ralf Kleppinger for providing us with the WAXD crystallinity, Jos Linsen for DMTA analysis, Harry Linssen for recording and analysis of ^{13}C NMR spectra of the PPR solution, and Daniel Johannson from Bodycote AB Sweden for performing the hydrostatic pressure test.

References

[1] Kimmich R. NMR—tomography, diffusiometry, relaxometry. Berlin: Springer; 1997.
[2] Spiess HW. Colloid Polym Sci 1983;261:193.
[3] Bilski P, Sergeev NA, Wasicki J. Mol Phys Rep 2000;29:55.
[4] Bilski P, Segreev NA, Wasicki J. Mol Phys 2003;101:335.
[5] Ailion DC. In: Waugh JS, editor. Advances in magnetic resonance. New York: Academic Press; 1971 vol 5, p. 177.
[6] Wunderlich B. Thermal analysis. San Diego: Academic Press.; 1990.
[7] The investigation on the relation of the onset temperature and the storage temperature has been performed in 1997 at the University of Erlangen in the group of Prof. Ehrenstein on behalf of the former Vestolen GmbH (now SABIC EuroPetrochemicals).
[8] Colquhoun IJ, Packer KJ. Br Polym J 1987;19:151.
[9] Clayden NJ. J Polym Sci, Part B: Polym Phys 1994;32:2321.
[10] Packer KJ, Poplett IJF, Taylor MJ. J Chem Soc, Faraday Trans 1 1988; 84:3851.
[11] Abragam A. The principles of nuclear magnetism. Oxford: Clarendon Press; 1961.
[12] Tanaka H. J Appl Polym Sci 1982;27:2197.
[13] Tanaka H, Kohrogi F, Suzuki K. Eur Polym J 1989;25:449.
[14] Tanaka H, Kohrogi F, Suzuki K. Angew Makromol Chem 1990;175:29.
[15] Tanaka H, Inoue Y. Eur Polym J 1993;29:569.
[16] Tanaka H, Inoue Y. Polym Int 1993;31:9.
[17] Dadauli D, Harris RK, Kenwright AM, Say BJ, Sünnetçioğlu MM. Polymer 1994;35:4083.
[18] Dujourdy L, Bazile JP, Cohen-Addad JP. Polym Int 1999;48:558.
[19] Schreurs S, François JP, Adriaensens P, Gelan J. J Phys Chem 1999; 103:1393.
[20] Weglarz WP, Peemoeller H, Rudin A. J Polym Sci, Part B: Polym Phys 2000;38:2487.
[21] VanderHart DL, Snyder CR. Macromolecules 2003;36:4813.
[22] Aharoni SM. Macromolecules 1983;16:1722.
[23] Wool RP. Macromolecules 1993;26:1564.
[24] Heymans N. Macromolecules 2000;33:4226.
[25] Douglass DC, McBrierty VJ, Weber TA. J Chem Phys 1976;64:1533.
[26] Douglass DC, McBrierty VJ, Weber TA. Macromolecules 1977;10: 178.
[27] Tanaka H, Saito K. Colloid Polym Sci 1988;266:1.
[28] Tanaka H, Takagi K. Br Polym J 1989;21:519.
[29] Ren W. Colloid Polym Sci 1992;270:747.
[30] Tanaka H. J Appl Polym Sci 1983;28:1707.
[31] McBrierty VJ, Packer KJ. Nuclear magnetic resonance in solid polymers. Cambridge: Cambridge University Press; 1993.
[32] Litvinov VM. In: Litvinov VM, De PP, editors. Spectroscopy of rubbers and rubbery materials. Shawbury: Rapra Technology Ltd; 2002. p. 353.
[33] Dórazio L, Mancarella C, Martuscelli E, Sticotti G, Ghisellini R. J Appl Polym Sci 1994;53:387.
[34] Nomura T, Nishio T, Fujii T, Sakai J, Yamamoto M, Uemura A, Kakugo M. Polym Eng Sci 1995;35:1261.
[35] Clayden NJ. Polymer 1992;33:3145.
[36] Tanzer CI, Roy AK. Proc SPE ANTEC'95 1995;95:2700–6.
[37] Dechene RL, Smith TB, Marino SAC, Tache RJ, Roy AK, USA Patent WO 96/21866; 1996.
[38] Litvinov VM, Barendswaard W, van Duin M. Rubber Chem Technol 1998;71:105.
[39] Isasi JR, Mandelkern L, Galante MJ, Alamo RG. J Polym Sci, Polym Phys Ed 1999;37:323.
[40] Litvinov VM, Mathot VBF. Solid State Nuclear Magn Reson 2002;22: 218.
[41] Barendswaard W, Litvinov VM, Souren F, Scherrenberg RL, Gondard C, Colemonts C. Macromolecules 1999;32:167.
[42] Litvinov VM, Mathot VBF. Solid State Nuclear Magn Reson 2002;22: 218.